AIAA 94-MSC

PASSIVE OPTICAL CUEING AND DISCRIMINATION OF THRUSTING THEATER MISSILES THROUGH CLOUD*

Ven H. Shui and Noel A. Thyson
Textron Defense Systems
201 Lowell Street, Wilmington, MA 01887

Abstract

The presence of cloud may delay electro-optical sensor boost plume detection and tracking until the target is above the cloud layers. This paper evaluates a technique that could eliminate or significantly reduce such time delays and assesses potential impacts on BPI CONOPS, BMC4I and weapon system performance, trade and optimization considerations.

1. Introduction

Boost phase intercept (BPI) of theater ballistic missile via an airplane-launched interceptor missile that delivers a kinetic-energy, hit-to-kill vehicle that intercepts the boosting threat has the advantage of containing warheads of mass destruction (nuclear, biological, and chemical) over hostile territory. In addition, an early intercept of the threat missile just after booster engine cut-off is still advantageous; if the intercept altitude is below about 70 km, the presence of the atmosphere will prevent the release of submunitions or decoys (fractionation) by the threat (see Figure 1).

A representative BPI architecture is illustrated in Figure 2. In its operational implementation, a threat missile will be detected within seconds after launch by an airborne optical sensor. Using the Joint Tactical Information Distribution System, this information is fused with other sensor and/or intelligence data. An initial intercept solution is formulated and intercept time and position are relayed to the selected interceptor launch aircraft. Within 15 to 25 seconds, the launch aircraft adjusts its heading, downloads time and positional data to the interceptor and fires the interceptor at the projected intercept point. In-flight target updates are periodically transmitted to the interceptor from the battle management and control system. After interceptor burn-out, its protective shroud is removed and the kinetic kill vehicle separates from the spent stage. Using a medium wave infrared seeker, the KKV uses divert thrusters and aerodynamic forces to guide it to a lethal collision. Kill assessment is performed by the airborne optical sensor and other sensors.

Table 1. Factors contributing to stressing BPI timelines

- Short engagement time $\leq$ 80 sec
- Reasonable stand-off required $\geq$ 150 km
- Early commit of interceptor $\leq$ 20 sec

As summarized in Table 1, BPI timelines are stressing, requiring detection, discrimination, and track establishment of threat missiles within seconds after launch. Passive electro-optical sensors on additional off-board aircraft platforms are ideal for this task due to their large field of view, high sensitivity, high resolution, rapid response, high data rate, and generally large range capabilities under clear air conditions. Although radar detection and tracking appears ideal for all-weather capability, the cost and number of airborne radar systems needed to give the large-area, long-range coverage are very high. Major airborne sensor functions required for the BPI mission are summarized in Table 2.

However, the presence of cloud introduces additional attenuation of the boost plume radiance and could preclude optical detection and tracking of the threat missile until it traverses the cloud layers. For most mission and engagement geometries, the slant path from the threat missile to the sensor through the cloud can be considerably longer than the vertical thickness of the cloud layer. The direct signal from the missile

* Paper for presentation at the AIAA Missile Science Conference, Monterey, California, November 7-9, 1994.

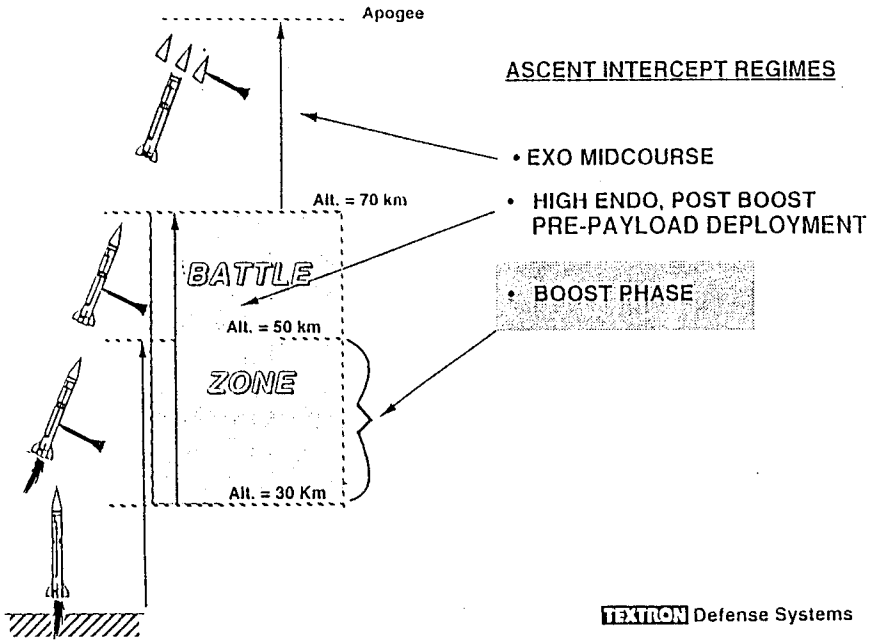

Figure 1. Boost phase intercept is the high-leverage TMD layer. Effective intercept altitude extends to about 70 km, where considerable atmosphere makes deployment of submunitions or decoys impractical.

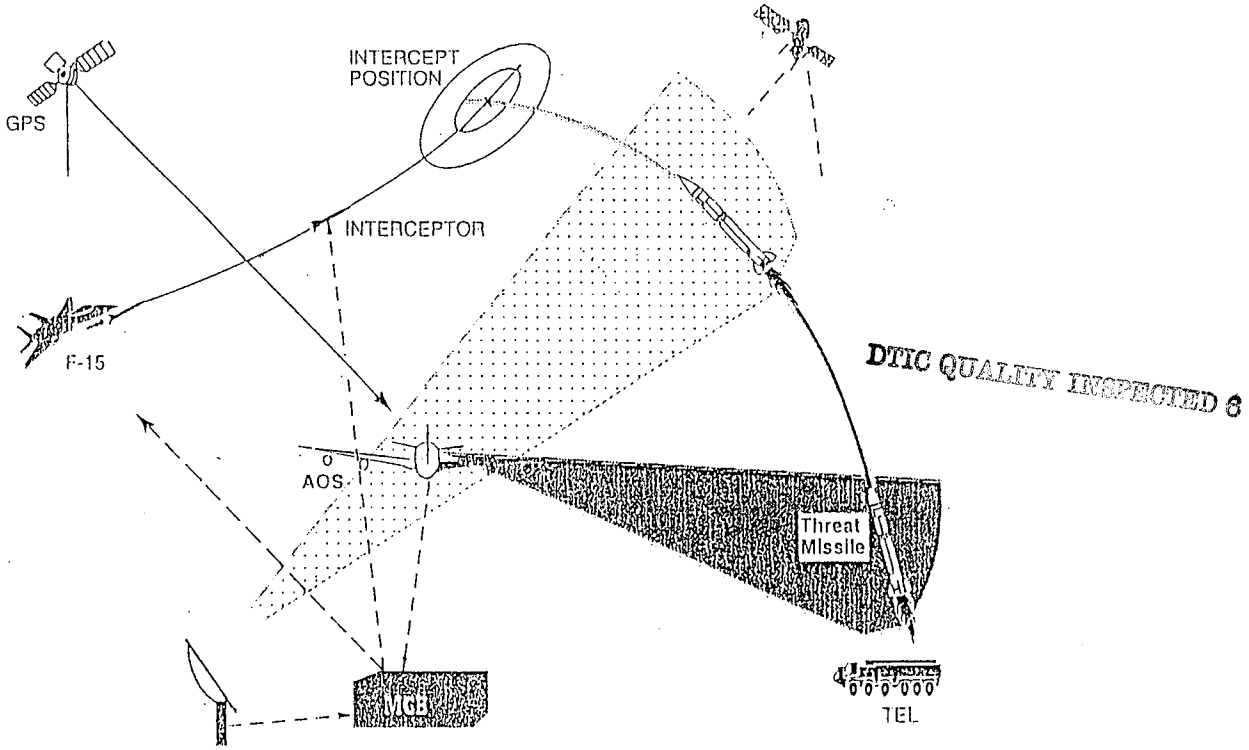

Figure 2. Representative BPI architecture illustrating major system elements.

plume to the sensor can become undetectable due to severe attenuation over the long slant path through the intervening cloud. As a result, intercept of the threat missile could be significantly delayed and the performance of the BPI mission could be seriously degraded. Figure 3 shows that achievable interceptor launch aircraft stand-off ranges can be significantly reduced by cloud-induced time delays. The reduction in stand-off is substantial for both BPI and pre-fractionation intercept at 70 km altitude, although the achievable standoff for prefractionation intercept is considerably larger than that for BPI.

Table 2. Major functions of the airborne sensor platform

- Mandatory on-board functions
  - Clutter rejection
  - Determination of viable threat missiles that are to be tracked
  - Typing of threat missiles
    - model based metric match
    - absolute intensity of plume
  - Calculations of potential intercept points in the boost phase and post-boost prefractionation battle space for each threat missile
  - Determination of each threat missile's current position
- It may be advantageous to also perform additional functions related to battle management aboard the airborne sensor platform

The present paper evaluates an approach that has the potential of significantly reducing or possibly eliminating such time delays. As illustrated in Figure 4, the approach relies on observing the residual electro-optical signal from the threat missile plume that propagates to the top of the cloud layer by multiple scattering. Our modeling approach, optical transport equations, solution approaches, and representative results of caculations will be described in Section 2. Potential impact on BPI CONOPS, BMC4I, and weapon system performance will be discussed in Section 3. A summary will appear in Section 4.

2. Modeling and Analysis

The scattering of a finite radiant source by an optically thin volume of particles can be evaluated by single-scattering approximations.[1-3] The scattered spectral irradiance is given by

$$E_v(\lambda) = I_s(\lambda) R^{-2} \exp[-(q_s - q_v)/\mu] \quad (1)$$

where $I_s(\lambda)$ is the source spectral radiant intensity, λ is the wavelength, R is the distance between the source and the scattering volume, q is the optical depth, and μ is the direction cosine from source to scattering volume. The spectral radiant intensity scattered toward a receiver is

$$I_v(\lambda) = E_v(\lambda)\, VP(\Phi), \quad (2)$$

where V is the scattering volume and $P(\Phi)$ is the scattering cross-section per unit volume per unit solid angle at scattering angle Φ. For propagation through optically thick clouds, multiple scattering and absorption must be taken into account. Numerical results can be obtained by making Monte Carlo calculations based on the aggregation of multiple independent single-photon paths.[4] Other approaches are based either on the wave equations[5] or on the transport theory[6]. Following the transport theory approach, the basic optical transport equations can be written as[7]

$$\nabla \cdot \hat{s} I(\vec{r}, \hat{s}) = \int \alpha \phi(\hat{s}, \hat{s}') I(\vec{r}, \hat{s}')\, d\omega' - I(\vec{r}, \hat{s}) + \epsilon(\vec{r}, \hat{s}) \quad (3)$$

where I(r,s) is the specific intensity,
- r is a position vector,
- s is a direction unit vector,
- α is the attennuation coefficient,
- ϕ is the phase function,
- ω is a solid angle, and
- ε is a source function.

Several approaches to solving Equation (3) have been reported in the literature. Examples include the diffusion approximation, the small-angle

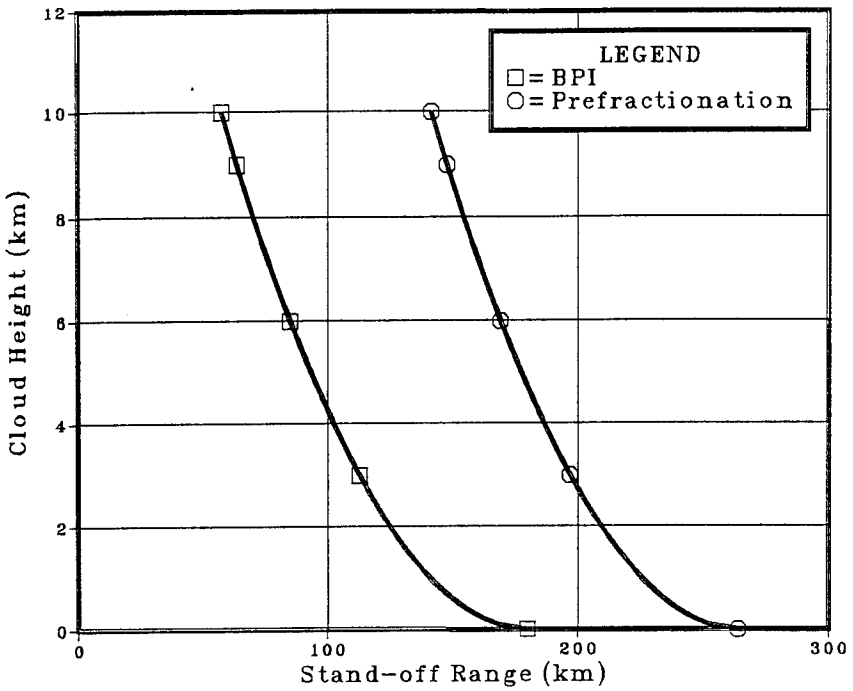

Figure 3. Achievable interceptor launch aircraft stand-off ranges can be significantly reduced by cloud-induced time delays. Stand-off ranges are considerably larger for pre-fractionation intercepts at 70 km altitude.

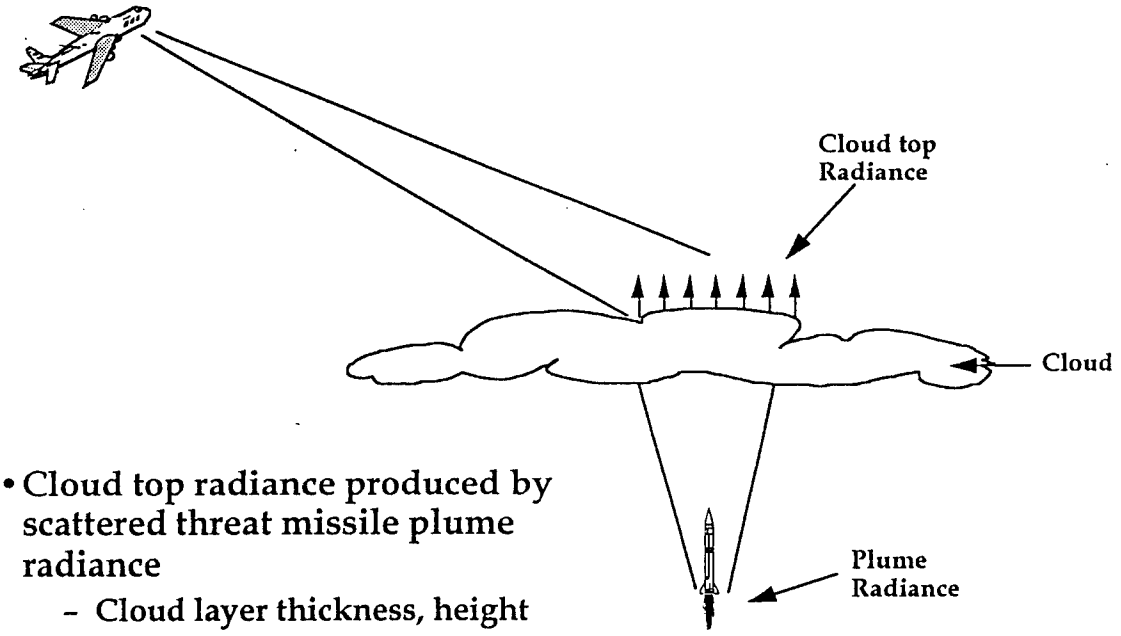

- Cloud top radiance produced by scattered threat missile plume radiance
  - Cloud layer thickness, height
  - Cloud water content, particle size
  - night and day operation

Figure 4. Passive optical detection/cueing/tracking in cloud.

approximation, multiple-stream approximation, and hybrid approximations. In addition, the well-known LOWTRAN series of computer codes can be used conveniently for many atmospheric propagation calculations. For the present investigation, we needed the additional ability and flexibility to model finite sources and to simulate clouds of arbitrary characteristics. This was accomplished by adapting available solutions and computer codes, and developing modified versions of the Monte Carlo models/codes[4,8] and multiple-stream models/codes.[7,9,10]

These modified models and computer codes have been used in our investigation and an example of the results is shown in Figure 5, which illustrates the level of photon flux available at the airborne sensor. In

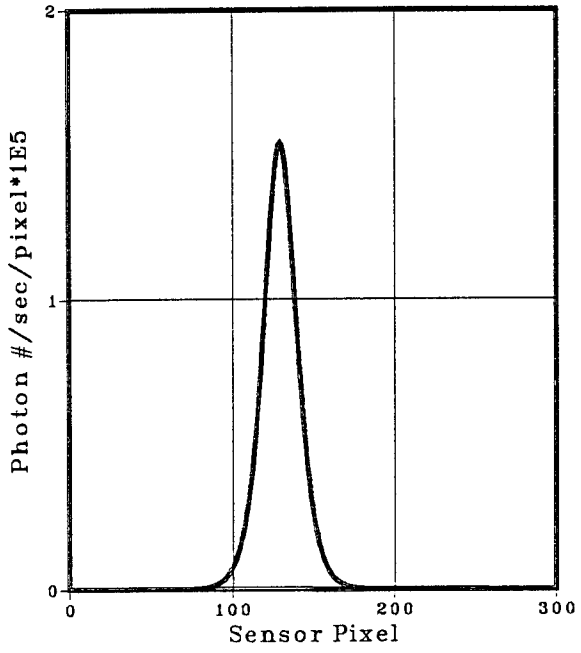

Figure 5. Residual cloud-top radiance can provide photon fluxes of order of 10^5 at sensor. 2 km thick, attenuation coefficient 20/km, see text for other conditions.

this hypothetical case, the source is at zero altitude with spectral radiant intensity 1.0E7 W/μm, the sensor is at 13 km altitude and 150 km range, and the cloud layer is 2 km thick with its top at 5 km altitude and has a total attenuation coefficient of 20/km. We note that in this case the photon flux level reaching the sensor from the residual radiance at the top of the cloud should be detectable by the sensor whereas the direct signal along the slant path from the source to the sensor is lower by over ten orders of magnitude and is not detectable.

3. Boost Phase Intercept Application Considerations

The impact of the presence of cloud and the associated time delays must be considered in the context of BPI CONOPS, BMC4I, and weapon system performance evaluation. For the BPI architecture described in Section 1, successful intercept of the threat missile requires numerous coordinated actions of all the system elements involved. Major timeline events/actions for BPI battle management and control are summarized in Table 3. Models and algorithms have been developed to simulate BPI mission/operation on the computer. The representative simulation flow diagram in Figure 6 illustrates some of the major modules involved. These simulations can be performed either completely on the computer or with pilot/operator and/or hardware in the loop. Models and results for cloud propagation and time delays can be incorporated into the appropriate modules.

As indicated earlier in Section 1 (see Table 2), the airborne sensor must perform several functions including clutter rejection and threat typing. Operational considerations demand that a large battlefield launch area be monitored by the the sensor effective field-of-view. As a result, in addition to backgroud clutter, numerous false targets are likely to be present in the sensor FOV and must be rejected and/or identified. These objects include: aircraft, antiaircraft/SAMs/ASMs, artillery/rockets, cruise missiles, fires, and solar reflections. A real-time prosessor is needed to perform these functions for the BPI mission.

Monitoring the characteristics of the residual plume radiant intensity at the top of the cloud may provide a basis for clutter rejection and discrimination. Primary features for this purpose are peak intensity, lateral size, and time/location history. Spectral data, if available, can further enhance performance. Calculations have been made for the hypothetical case described in Section 2. The resulting peak intensity is plotted versus target altitude in Figures 7. Figure 8 illustrates the change in radiance intensity at the top of the cloud as a function of cloud layer thickness. Following are several examples of the specific approaches that illustrate the use of our models, algorithms, and predictions as a decision aid for BPI BMC4I.

Table 3. Boost phase intercept battle management and control major events/actions/timeline.

	Time	Event/Action
(1)		AOS monitors battle area, rejecting clutter and non-viable threats.
(2)		Threat TBM is launched and is detected by AOS as viable threat.
3.		AOS makes initial estimate of threat launch point position.
4.		AOS types threat.
5.		AOS makes initial estimate of BECO position and time.
6.		BM determines feasibility of F-15/interceptor on CAP for BPI, Post Boost PFPI or no intercept.
7.		BM selects F-15 for BPI or PFPI.
8.		BM selects az or az-el launch & sends initial az-el to F-15.
9.		F-15 begins maneuver to az-el.
10.		BM sends final update az-el to F-15.
11.		BM sends to F-15 intercept point location, time, error basket and gives order to launch.
(12)		F-15 reaches desired az-el, transfers alignment and target intercept position/time to interceptor, and launches interceptor.
(13)		AOS continuously updates target info to BM, BM continuously updates intercept point info to interceptor throughout 1st Stage and 2nd Stage burns.
(14)		Shroud removal after 2nd Stage burnout.
15.		KKV deployment
16.		AOS/BM sends current target position to KKV, KKV adjusts attitude, seeker orientation, and acquires target (plume).
17.		KKV performs midcourse homing diverts (plume) to intercept target.
18.		KKV performs endgame homing diverts (plume/hardbody transition and aimpoint selection) to intercept target.
(19)		KKV intercepts threat.
20.		AOS and other assets perform kill assessment.

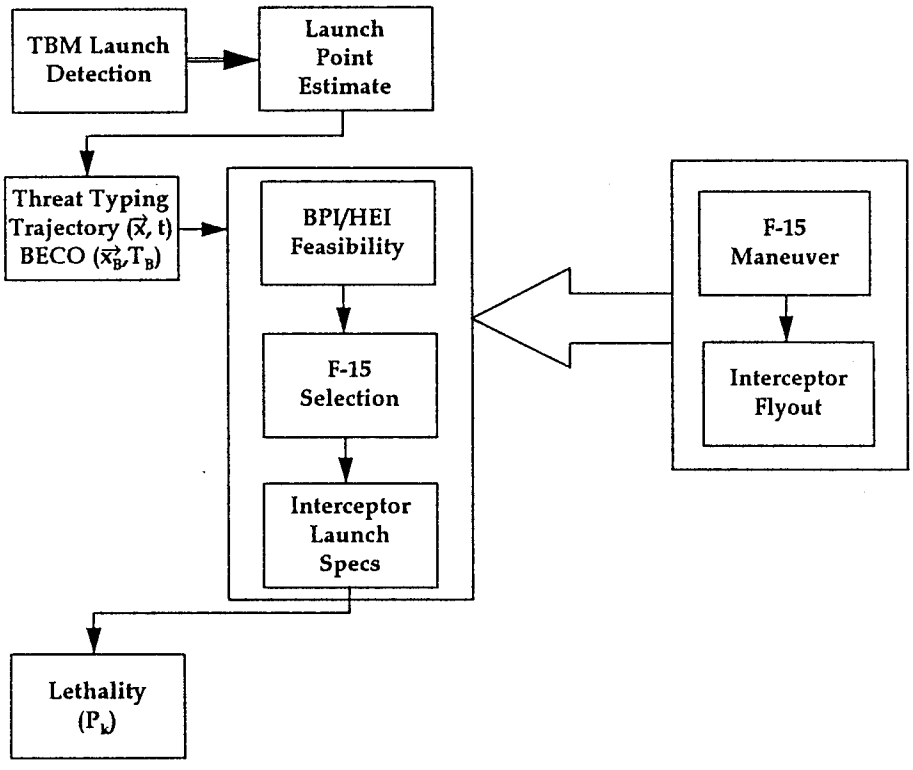

Figure 6. Boost phase intercept simulation models/algorithms.

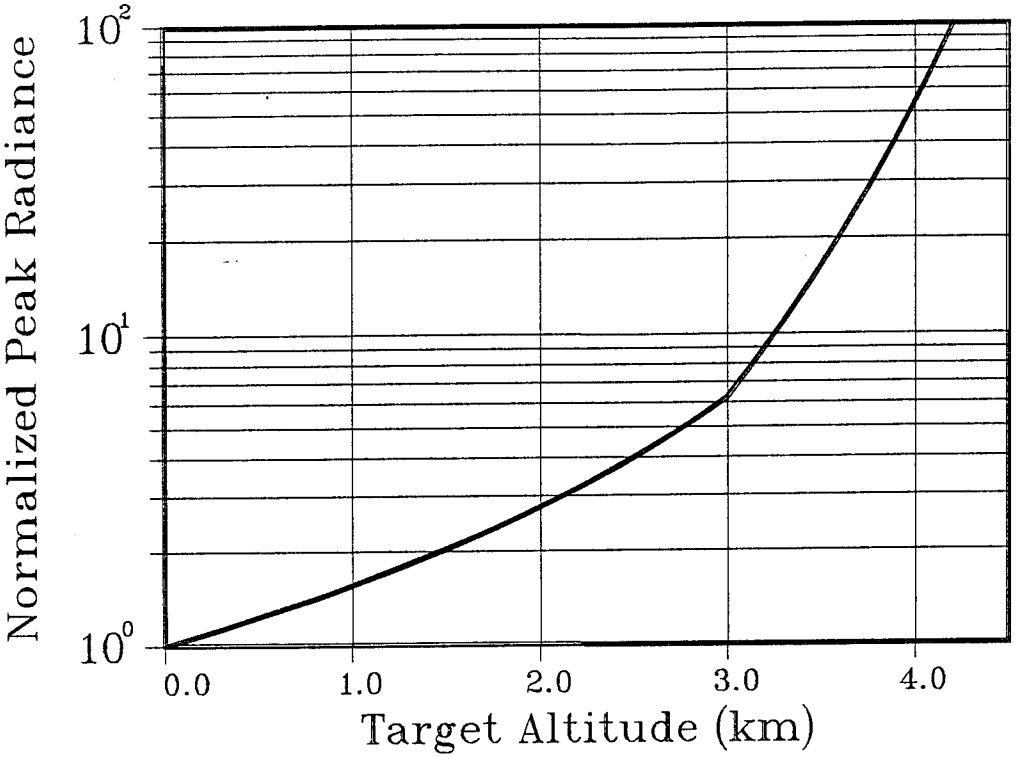

Figure 7. Variation of cloud-top radiance with target altitude for 2 km thick cloud with top at 5 km altitude.

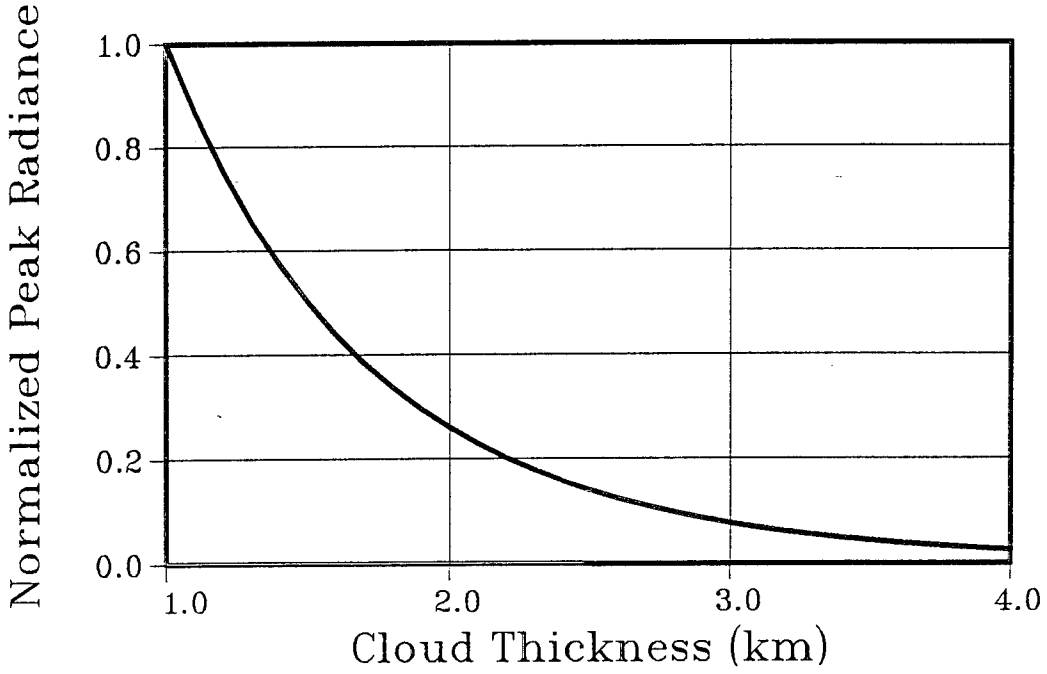

Figure 8. Variation of cloud-top radiance with cloud thickness. Base of cloud layer is at 1 km altitude. Source is at ground level.

a) After the cloud-top radiance is observed by the passive, large-FOV sensor, their ranges from the sensor platform can be estimated by correlation with sensor platform altitude, attitude, and cloud data. This allows the construction of an absolute-intensity distribution map, which can then be used as a basis for discrimination and cueing.

b) Initial passive sensor results can be used to direct the operation of an on-board range-finder to obtain more accurate ranges, more accurate intensities, and consequently more reliable discrimination and cueing. It should be noted that range-finder operations are in general more time consuming and a trade-off is needed for optimization.

c) Time histories of the intensity patterns (level, size, location, continuity) can be used to further enhance discrimination and cueing. For example, TBMs and SAMs tend to have markedly different flyout profiles and burn times.

d) For situations where signal-to-background ratio is relatively low, multiple-frame processing and MTI techniques can be incorporated to enhance target extraction. Spectral data, if available, and wavelength tradeoff/optimization can further improve performance.

Work is in process to carry out additional calculations for specific engagement cases, to incorporate the results/correlations into the real-time processor and into the BPI system simulations, to assess effects of cloud characteristics, and to consider experimental verification/calibration.

4. Summary

Direct detection of boost plume by an airborne EO sensor through cloud is usually not possible due to the severe attenuation caused by propagation through the long slant-path between the plume and the sensor. The vertical path to the top of the cloud layer is considerably shorter. Multiple-scattering model and calculations show that the residual radiance at the top of the cloud would provide high levels of photon flux at the sensor and detection is feasible. Furthermore, monitoring the characteristics and time history of this residual radiance may provide a basis for clutter rejection and discrimination. Preliminary analyses of the processor models/algorithms and BPI system simulations indicate potentially substantial weapon system performance improvements such as achievable interceptor launch aircraft standoffs.

References

1. H. C. van de Hulst, Light Scattering By Small Particles, Wiley, 1957.

2. M. Born and E. Wolf, Principles of Optics, Pergaman, 1959.

3. M. Kerker, The Scattering of Light, Academic, 1969.

4. G. N. Plass and G. W. Kattawar, "Monte Carlo calculations of light scattering from clouds", Appl. Optics Vol 7, 415 (1968).

5. V. Twersky, "On propagation in random media of discrete scatterers", Proc Am Math Soc Symp Stochas Proc Math Phys Eng Vol 16, 84 (1964).

6. S. Chandrasekhar, Radiation Transfer, Oxford UP, 1950.

7. A. Ishimaru, Wave Propagation and Scattering in Random Media, Academic, 1978.

8. V. H. Shui, "Monte Carlo trajectory calculations of three-body recombination and dissociation of diatomic molecules", J. Chem. Phys. Vol 57, 1972.

9. W. L. Wolfe and G. J. Zissis, editors, The Infrared Handbook, ERIM, 1978.

10. R. G. Isaacs, W. C. Wang, R. D. Worsham, and S. Goldberg, "Multiple scattering LOWTRAN and FASCODE models", Applied Optics, Vol 26, 1272 (1987).